NACA RM L50A18

NACA

RESEARCH MEMORANDUM

AERODYNAMIC CHARACTERISTICS OF A WING WITH UNSWEPT QUARTER-CHORD LINE, ASPECT RATIO 2, TAPER RATIO 0.78, AND NACA 65A004 AIRFOIL SECTION

TRANSONIC-BUMP METHOD

By Edward C. Polhamus and George S. Campbell

Langley Aeronautical Laboratory
Langley Air Force Base, Va.

NATIONAL ADVISORY COMMITTEE
FOR AERONAUTICS

WASHINGTON

March 8, 1950

NATIONAL ADVISORY COMMITTEE FOR AERONAUTICS

RESEARCH MEMORANDUM

AERODYNAMIC CHARACTERISTICS OF A WING WITH UNSWEPT QUARTER-CHORD LINE, ASPECT RATIO 2, TAPER RATIO 0.78, AND NACA 65A004 AIRFOIL SECTION

TRANSONIC-BUMP METHOD

By Edward C. Polhamus and George S. Campbell

SUMMARY

The aerodynamic characteristics of a low-aspect-ratio wing have been investigated in the Langley high-speed 7- by 10-foot tunnel over a Mach number range of 0.60 to 1.17 by use of the transonic-bump technique. The results include lift, drag, pitching-moment, and root bending moment for a wing having an unswept quarter-chord line, aspect ratio 2, taper ratio 0.78, and an NACA 65A004 airfoil section.

The variations of aerodynamic characteristics with Mach number in the low-lift range were relatively small except for a sudden 9-percent mean aerodynamic chord rearward movement of the aerodynamic center near a Mach number of unity.

Theoretical values of lift-curve slope and lateral center of pressure have been shown to be in good agreement with experimental results for subsonic Mach numbers. A comparison of the drag data with theory indicated that the high values of drag due to lift were probably caused by a loss in leading-edge suction.

INTRODUCTION

A series of wing and wing-fuselage combinations is being investigated in the Langley high-speed 7- by 10-foot tunnel to study the effects of wing geometry on longitudinal stability characteristics at transonic speeds. By utilizing the transonic-bump technique a Mach number range of about 0.60 to 1.18 is obtained.

This paper presents the results of an investigation of force and moment characteristics for a wing with an unswept quarter-chord line, aspect ratio 2, taper ratio 0.78, and an NACA 65A004 airfoil section parallel to the free stream.

MODEL AND APPARATUS

The semispan wing model of the present tests had an unswept quarter-chord line, an aspect ratio of 2, a taper ratio of 0.78, and an NACA 65A004 airfoil section parallel to the free stream. A two-view drawing of the wing, which was made of beryllium copper, is presented in figure 1; airfoil ordinates are given in table I. The wing was obtained by modifying an unswept wing having an aspect ratio of 4 and a taper ratio of 0.6 that was previously tested as part of the transonic research program. Pictorial views of the model mounted on the bump are presented in figures 2 and 3.

The model was mounted on an electrical strain-gage balance enclosed within the bump. The lift, drag, pitching-moment, and root bending moment were measured with potentiometers.

COEFFICIENTS AND SYMBOLS

C_L	lift coefficient (Twice panel lift/qS)
C_D	drag coefficient (Twice panel drag/qS)
C_m	pitching-moment coefficient referred to $0.25\bar{c}$ (Twice panel pitching moment/$qS\bar{c}$)
C_B	bending-moment coefficient about root chord line $\left(\text{Root bending moment}\Big/q\frac{S}{2}\frac{b}{2}\right)$
ΔC_D	drag coefficient due to lift $\left(C_D - C_{D_o}\right)$
q	effective dynamic pressure over span of model $\left(\rho V^2/2\right)$
ρ	air density
V	free-stream velocity
S	twice wing area of semispan model, 11.11 square inches

$\bar{c}$ mean aerodynamic chord of wing using theoretical tip $\left(\frac{2}{S}\int_0^{b/2} c^2 dy\right)$

c local wing chord

y spanwise distance from wing root

b twice span of model

A aspect ratio of wing $\left(b^2/S\right)$

X distance along airfoil chord, percent chord

Y airfoil ordinate, percent chord

M effective Mach number over span of model

M_a average chordwise local Mach number

R Reynolds number of wing based on $\bar{c}$

α angle of attack, degrees

y_{cp} lateral center of pressure, percent semispan $\left(100\frac{C_B}{C_L}\right)$

Subscripts:

M at a constant Mach number

l local value

o at zero lift

TESTS

The tests were conducted in the Langley high-speed 7- by 10-foot tunnel utilizing an adaptation of the NACA wing-flow technique for obtaining transonic speeds. The method used involves mounting a model in the high-velocity flow field generated over the curved surface of a bump located on the tunnel floor. (See reference 1.)

Typical contours of the local Mach number in the region of the model location on the bump, obtained from surveys with no model in position, are shown in figure 4. The spanwise Mach number gradient for the model tested increases from 0.02 at low Mach numbers to 0.04 at the higher speeds. The chordwise Mach number gradient is generally less than 0.02. No attempt has been made to evaluate the effect of these spanwise and chordwise variations of Mach number. The dash lines shown near the wing root represent a local Mach number 5 percent below the maximum value and indicate the extent of the bump boundary layer. The effective Mach number was obtained from contour charts similar to those presented in figure 4 from the relationship

$$M = \frac{2}{S}\int_0^{b/2} cM_a \, dy$$

The variation of test Reynolds number with Mach number is shown in figure 5.

Force and moment data were obtained for the model configuration tested through a Mach number range of 0.60 to 1.17 and an angle-of-attack range of -2° to 10°.

A cut out in the bump surface to allow changes in angle of attack during test runs necessitated use of an end plate to prevent leakage (fig. 2). Allowance for end-plate clearance exposed about 1/16 inch of the wing butt to the air stream. Since the exposed portion of the butt was well within the boundary layer (fig. 4), the effect on forces and moments is assumed small.

The end-plate tares on drag were obtained through the test Mach number range at zero angle of attack by testing the model configuration without an end plate. For this test, the same gap of about 1/16 inch was maintained between the wing root and the bump surface, and a sponge-wiper seal was fastened to the wing butt beneath the surface of the bump to prevent leakage (fig. 3). Tests of other bump models showed that the end-plate tares were practically invariant with angle of attack. Hence, the tares obtained at zero angle of attack were applied to all drag data. Jet-boundary corrections have not been evaluated since the boundary conditions to be satisfied are not rigorously defined. However, inasmuch as the effective flow field is large compared with the span and chord of the model, these corrections are believed to be small.

RESULTS AND DISCUSSION

The force and moment data are presented in figure 6. The summary of aerodynamic characteristics throughout the test Mach number range is shown in figure 7. Unless otherwise noted, the discussion is based on this summary. The slopes through zero lift have been averaged over a lift-coefficient range of ±0.1.

Lift and Drag Characteristics

The lift-curve slope increased gradually with Mach number from a value of 0.045 at a Mach number of 0.60 to the value of 0.055 at a Mach number of about 1.0. Values of theoretical lift-curve slope, as given in reference 2, using the Weissinger method and the three-dimensional Prandtl-Glauert transformation are shown (fig. 7) to be in good agreement with experimental results throughout the subsonic range tested. The value of theoretical lift-curve slope was calculated at sonic speed from the value of $\frac{1}{57.3}\left(\frac{\pi A}{2}\right)$ given in reference 3.

The lateral center of pressure was located at 42 percent of the semispan at a Mach number of 0.60. This value is essentially in agreement with the theoretical value obtained from reference 2. The lateral shift in loading with Mach number is observed to be small throughout the Mach number range of the present tests.

It is seen from figure 7 that the drag rise with Mach number is relatively small. However, the results indicate that the drag due to lift is approximately twice the theoretical value for full leading-edge suction (reference 2). In fact, the parameter $\Delta C_D/C_L{}^2$ approaches the theoretical value for zero leading-edge suction $\left(\frac{1}{57.3\left(\frac{\partial C_L}{\partial \alpha}\right)_M}\right)$. The expression for zero leading-edge suction results from the fact that with no leading-edge suction, the resultant force is normal to the chord line rather than the relative wind. Experimental lift-curve slope was used to compute the drag-due-to-lift parameter for zero leading-edge suction. The results indicate that this thin wing, having a relatively sharp leading edge, develops very little leading-edge suction, causing high drag due to lift.

Pitching-Moment Characteristics

Near zero lift coefficient, the aerodynamic center was at the quarter-chord at a Mach number of 0.60. The aerodynamic center gradually

shifted forward to 20 percent of the mean aerodynamic chord at high subsonic speeds. Between a Mach number of 0.98 and 1.03, the aerodynamic center moved rearward to the 29-percent point and remained nearly constant at the higher Mach numbers tested. It is noted from figure 6 that the aerodynamic center moved rearward at higher lifts, particularly at the higher Mach numbers.

CONCLUSIONS

The results of an investigation of a thin, unswept wing of low aspect ratio indicate the following:

1. The variations of the aerodynamic characteristics with Mach number in the low-lift range were relatively small except for a sudden 9-percent mean aerodynamic chord rearward movement of the aerodynamic center near a Mach number of 1.0.

2. Available theory satisfactorily predicted lift-curve slope and lateral center of pressure throughout the subsonic Mach number range.

3. Although the drag rise with Mach number was relatively small, the drag due to lift was high, apparently due to a loss in leading-edge suction.

Langley Aeronautical Laboratory
National Advisory Committee for Aeronautics
Langley Air Force Base, Va.

REFERENCES

1. Schneiter, Leslie E., and Ziff, Howard L.: Preliminary Investigation of Spoiler Lateral Control on a 42° Sweptback Wing at Transonic Speeds. NACA RM L7F19, 1947.

2. DeYoung, John: Theoretical Additional Span Loading Characteristics of Wings with Arbitrary Sweep, Aspect Ratio, and Taper Ratio. NACA TN 1491, 1947.

3. Spreiter, John R.: Aerodynamic Properties of Slender Wing-Body Combinations at Subsonic, Transonic, and Supersonic Speeds. NACA TN 1662, 1948.

TABLE I

NACA 65A004 AIRFOIL ORDINATES

[Percent chord]

X	Y
0	0
.5	.311
.75	.378
1.25	.481
2.5	.656
5.0	.877
7.5	1.062
10	1.216
15	1.463
20	1.649
25	1.790
30	1.894
35	1.962
40	1.996
45	1.996
50	1.952
55	1.867
60	1.742
65	1.584
70	1.400
75	1.193
80	.966
85	.728
90	.490
95	.249
100	.009
Leading-edge radius = 0.102 Trailing-edge radius = 0.010	

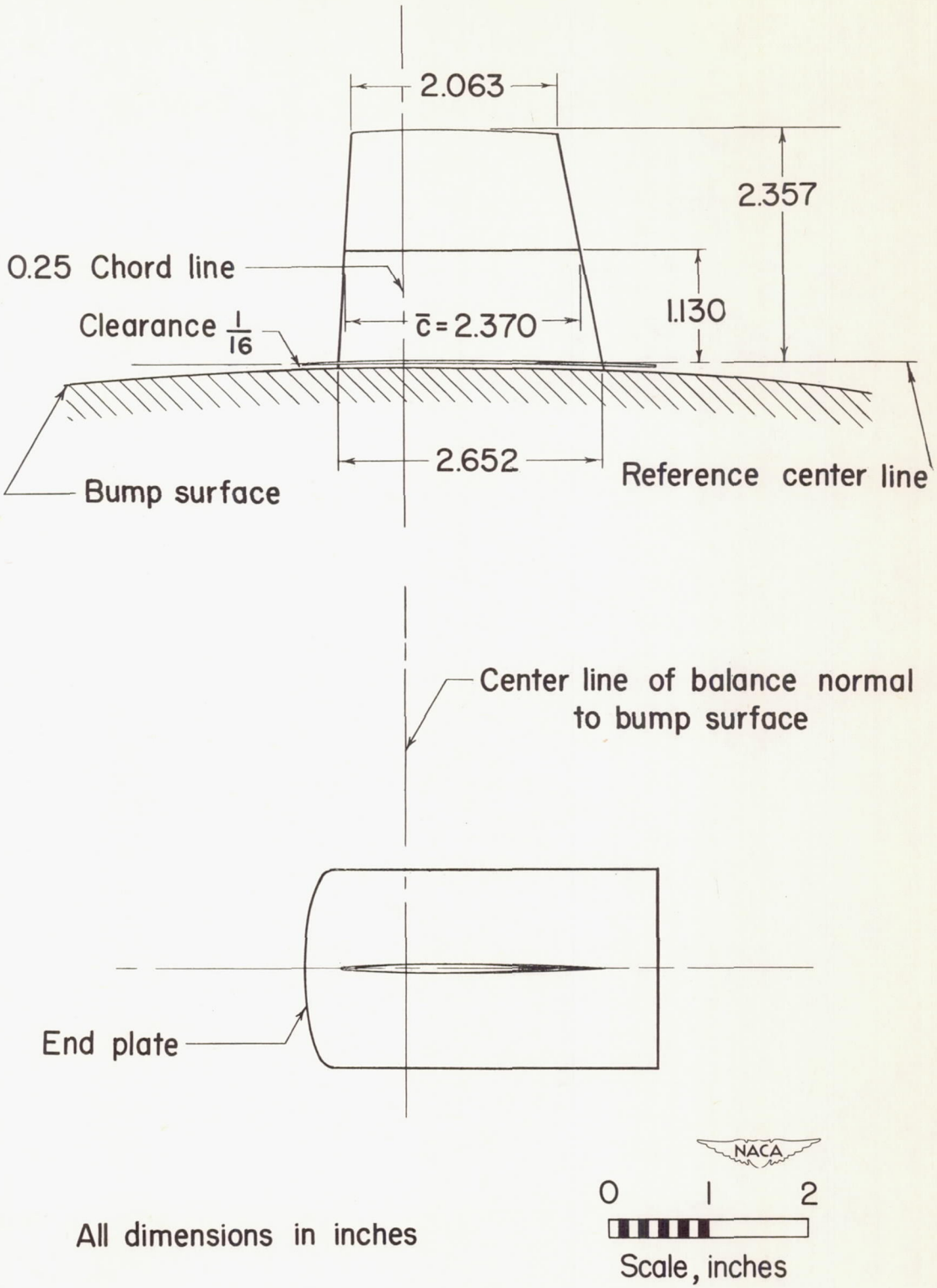

Figure 1.- General arrangement of model with unswept quarter chord, aspect ratio 2, taper ratio 0.78, and NACA 65A004 airfoil.

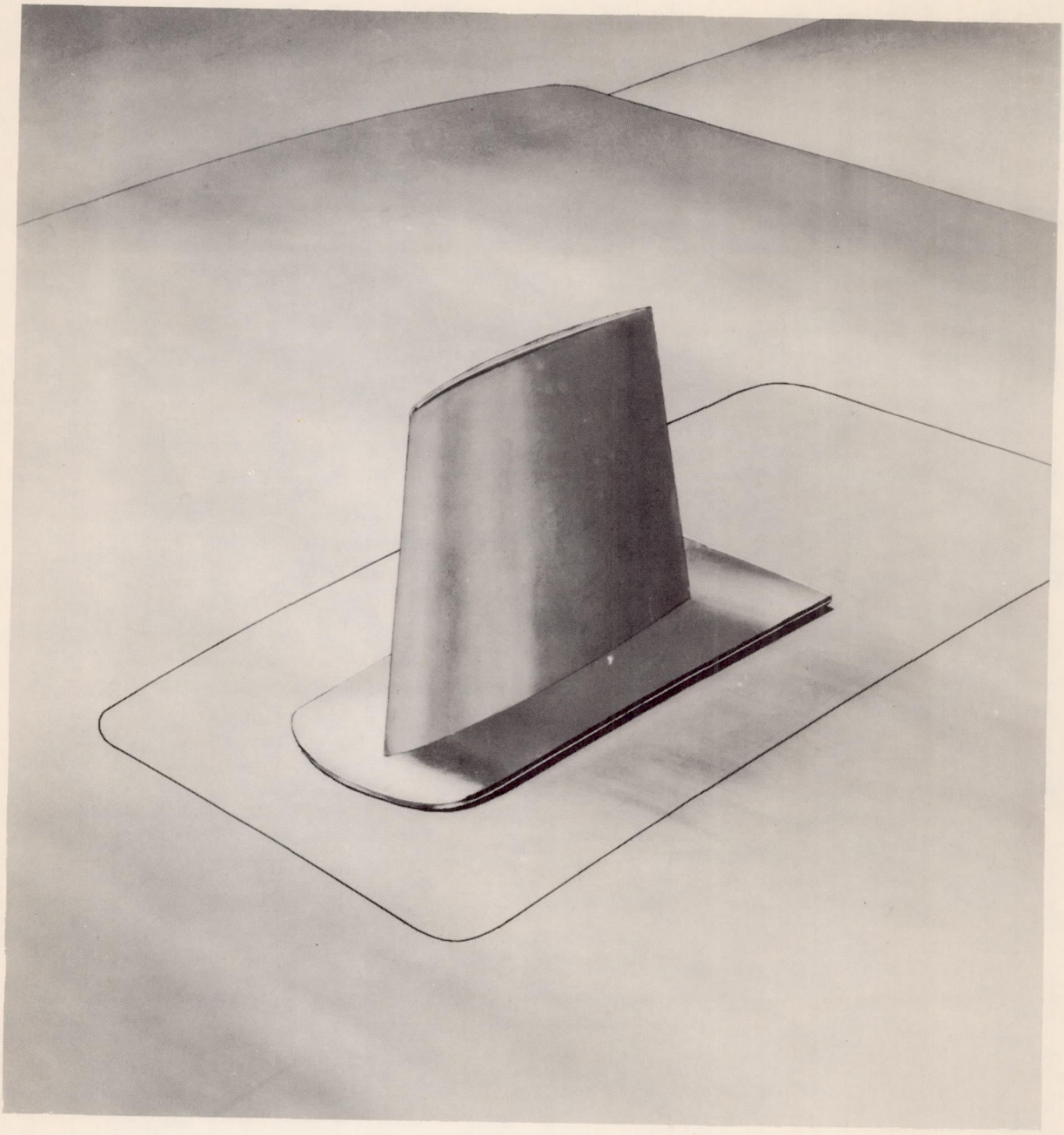

Figure 2.- Pictorial view of wing model and end plate mounted on the bump.

NACA

L-63786

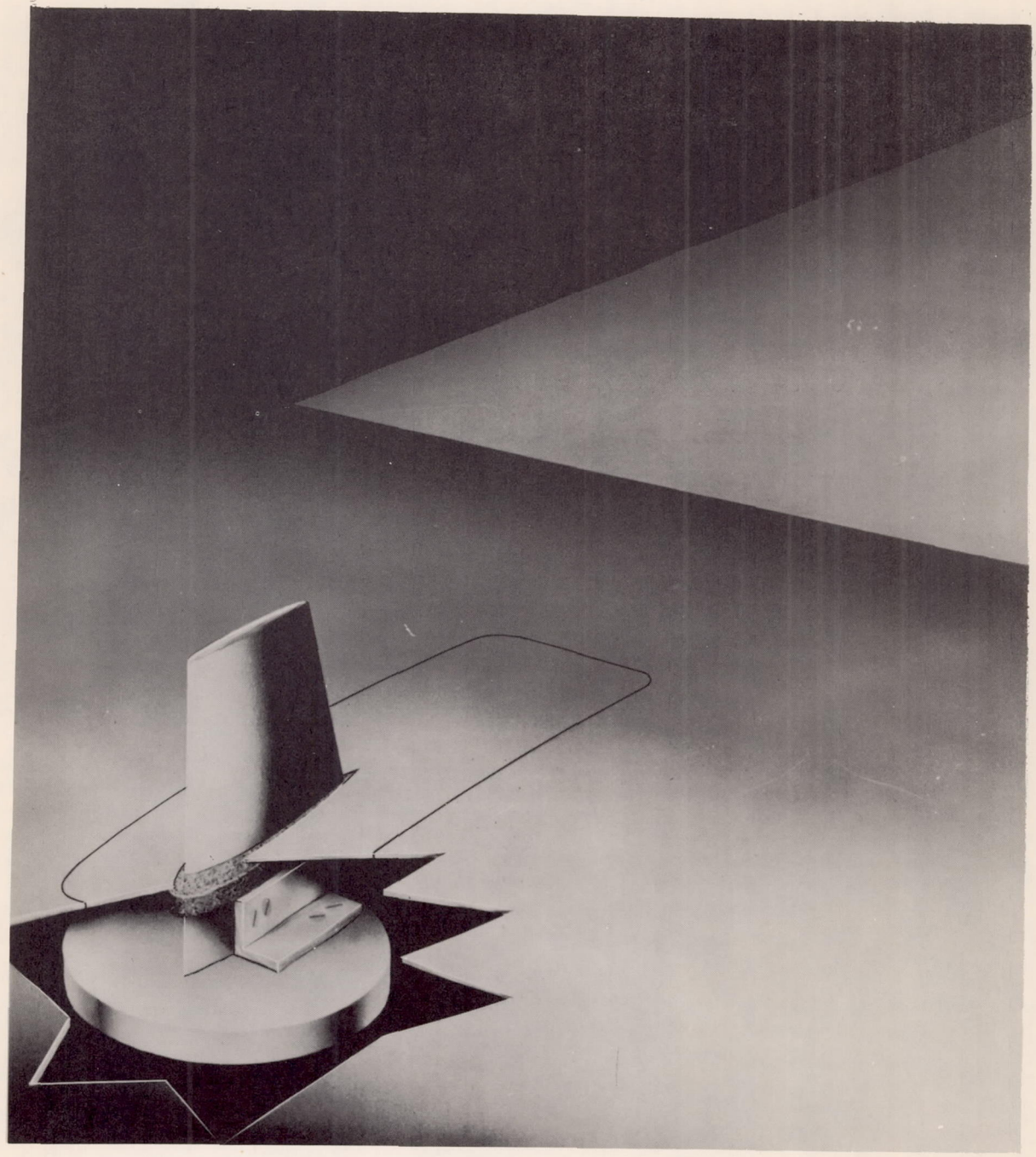

Figure 3.- Pictorial view showing sponge-wiper seal installation on the model. $\alpha = 0^{\circ}$.

NACA

L-62922

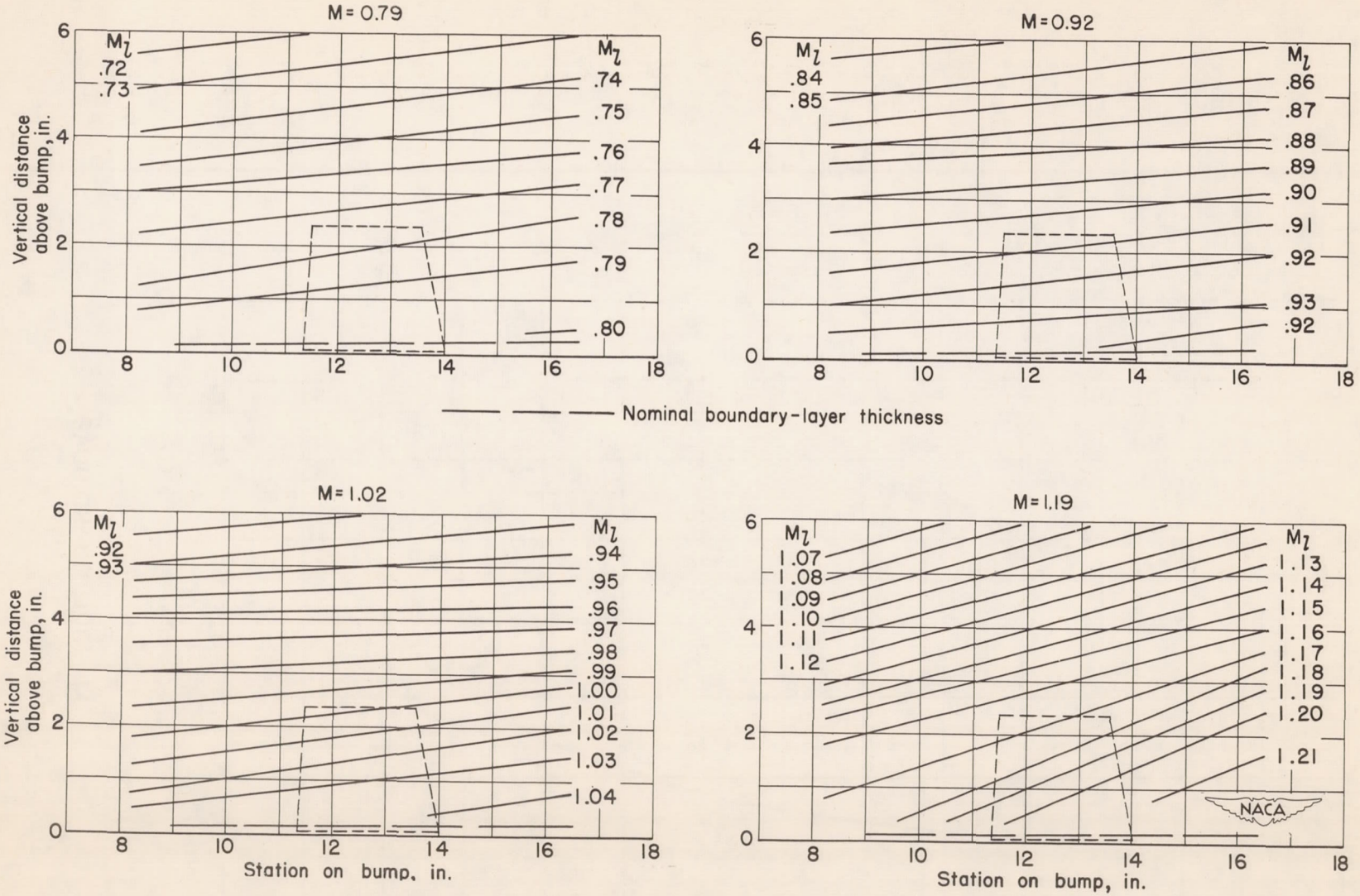

Figure 4.- Typical Mach number contours over transonic bump in region of model location.

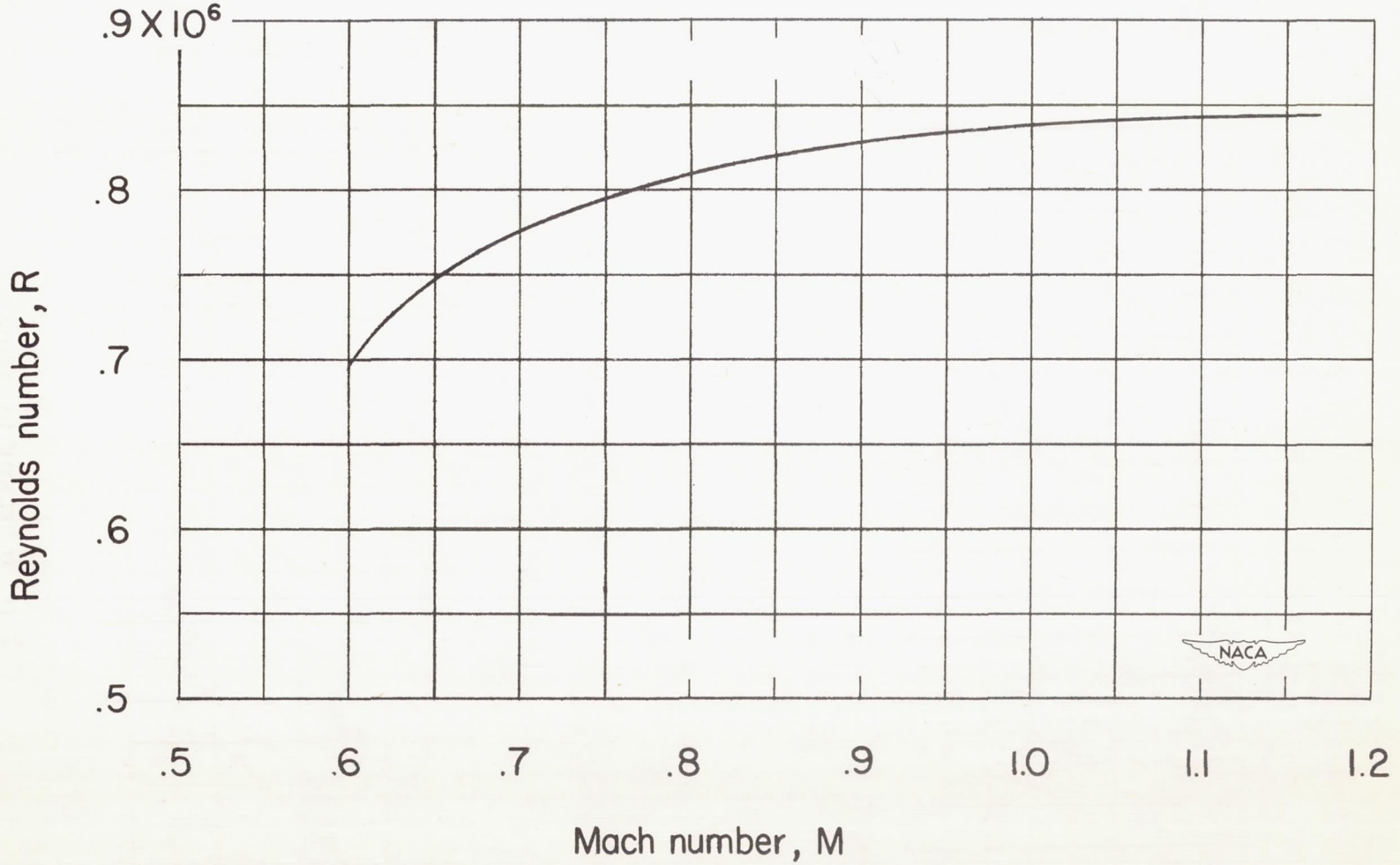

Figure 5.- Variation of test Reynolds number with Mach number for a model with unswept quarter chord, aspect ratio 2, taper ratio 0.78, and NACA 65A004 airfoil.

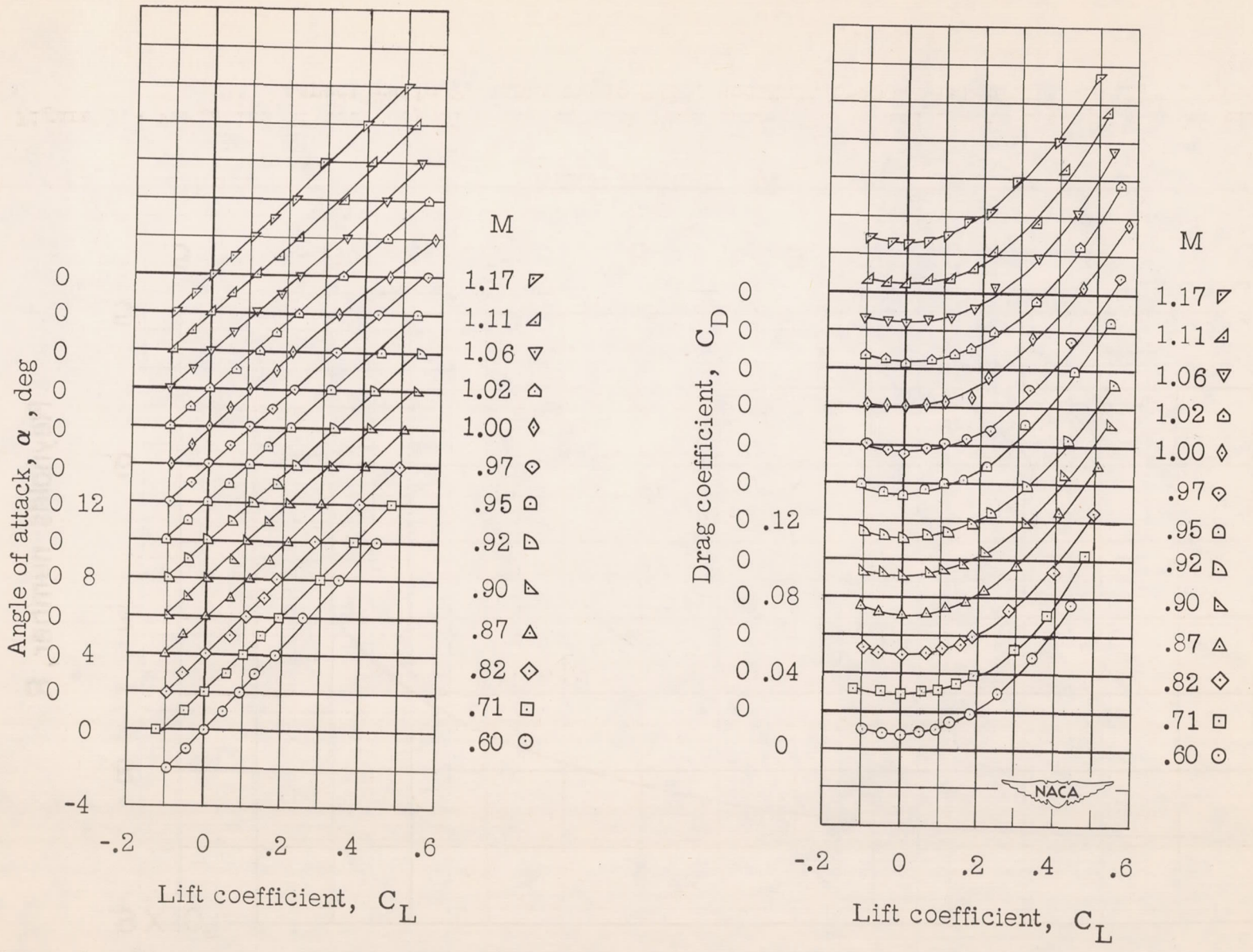

Figure 6.- Aerodynamic characteristics for a model with unswept quarter chord, aspect ratio 2, taper ratio 0.78, and NACA 65A004 airfoil.

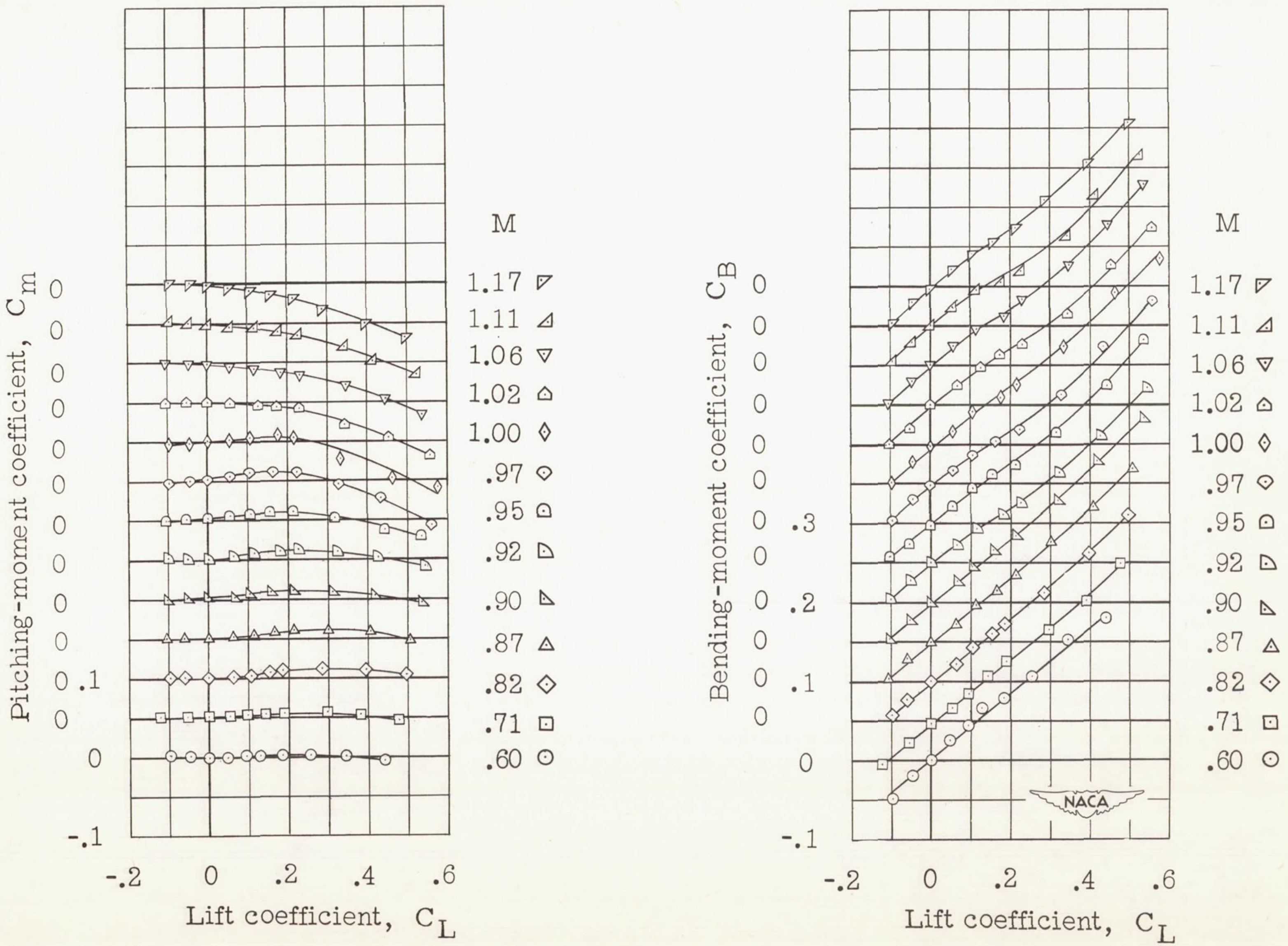

Figure 6.- Concluded.

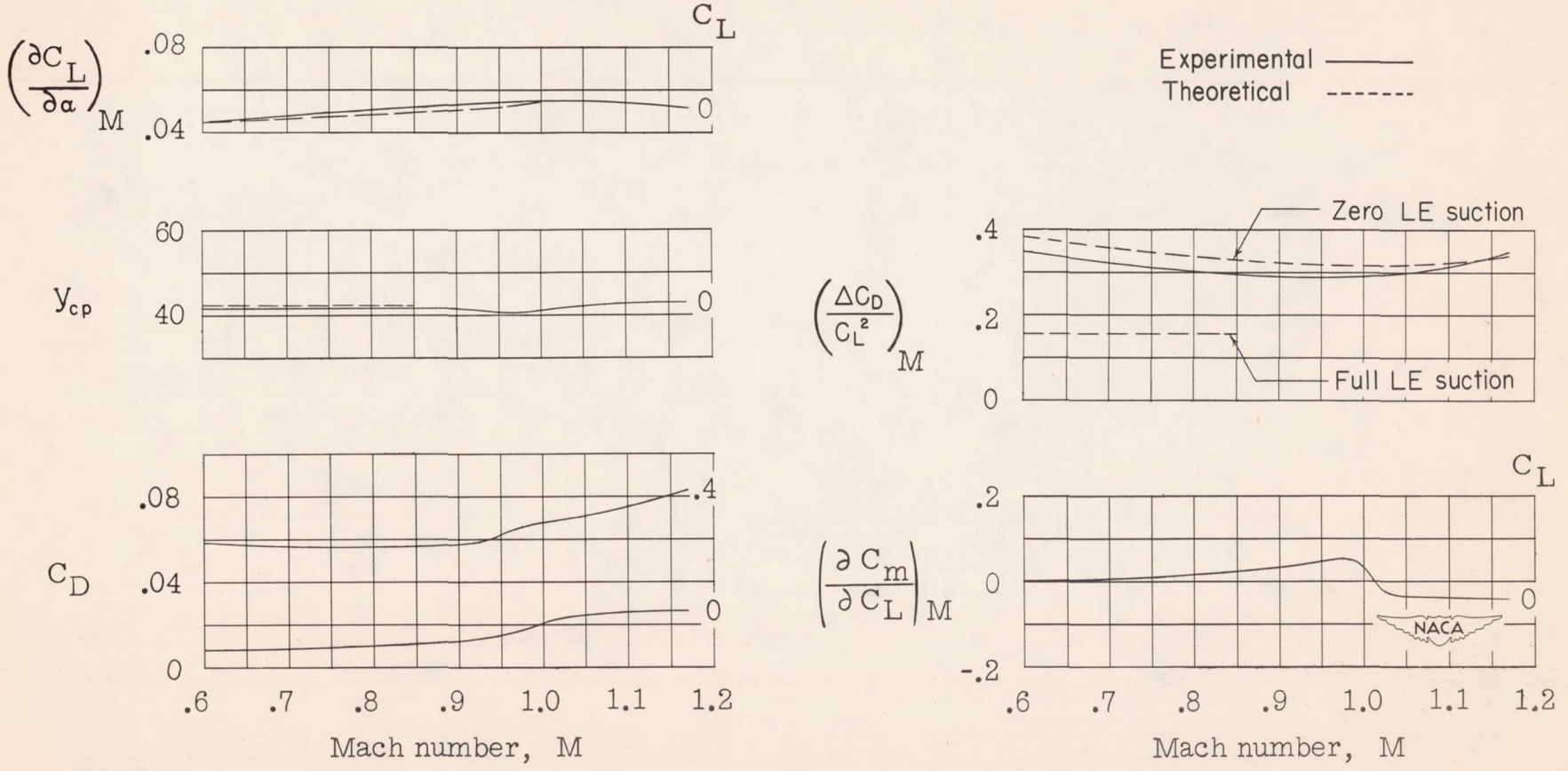

Figure 7.- Summary of aerodynamic characteristics for a model with unswept quarter chord, aspect ratio 2, taper ratio 0.78, and NACA 65A004 airfoil.